Clinical and Imaging Characteristics of *PRPH2* Retinopathies in a Longitudinal Cohort and Diagnostic Implications

Johanna M. Seddon,[1] Dikha De,[1] Laura Grunenkovaite,[1] and Daniela Ferrara[2,3]

[1]Department of Ophthalmology and Visual Sciences, University of Massachusetts Chan Medical School, Worcester, Massachusetts, United States
[2]Department of Ophthalmology, Tufts University School of Medicine, Boston, Massachusetts, United States
[3]Roche Personalized Healthcare, Genentech, Inc., South San Francisco, California, United States

Correspondence: Johanna M. Seddon, Department of Ophthalmology and Visual Sciences, University of Massachusetts Chan Medical School, 281 Lincoln St., Worcester, MA 01605, USA; johanna_seddon@yahoo.com.

Received: January 29, 2024
Accepted: November 3, 2024
Published: December 18, 2024

Citation: Seddon JM, De D, Grunenkovaite L, Ferrara D. Clinical and imaging characteristics of *PRPH2* retinopathies in a longitudinal cohort and diagnostic implications. *Invest Ophthalmol Vis Sci.* 2024;65(14):31. https://doi.org/10.1167/iovs.65.14.31

Purpose. The purpose of this study was to define genotypic-phenotypic correlations related to *PRPH2*-associated retinopathies in an observational longitudinal cohort and to improve diagnostic accuracy.

Methods. Individuals with *PRPH2* variants were identified by genetic sequencing of 263 individuals (including 59 families). Ocular examinations with multimodal imaging were evaluated.

Results. Two pathogenic/likely pathogenic *PRPH2* variants were identified in 22 individuals with retinopathies, low genetic susceptibility to age-related macular degeneration (AMD) and younger age of onset. The mean follow-up was 14 years. One family and 4 independent cases ($n = 7$) were heterozygous for the variant rs121918563 L185P (p.Leu185Pro). The individuals developed retinopathy compatible with autosomal dominant pattern dystrophy (PD), including adult-onset vitelliform macular dystrophy and butterfly macular dystrophy in their fourth to fifth decades of life, evolving to retinal pigment epithelial (RPE) irregularities and central macular atrophy 20 years later. Two families and an independent case ($n = 15$) had the rs281865373 splice-site variant c.828+3A>T (IVS2+3A>T) presenting as retinal flecks consistent with adult-onset fundus flavimaculatus with macular dystrophy and diffuse RPE atrophy consistent with central areolar chorioretinal dystrophy (CACD) in the fifth decade of life progressing to extensive atrophy in the sixth to eighth decades. The L185P variant was associated with better visual acuity (VA) during follow-up versus c.828+3A>T variant. Some individuals were initially misdiagnosed with geographic atrophy secondary to AMD.

Conclusions. Individuals with the L185P variant had less severe disease with clinical manifestation typical of PD and better VA. More advanced disease with CACD and worse VA were associated with the c.828+3A>T variant. Results contribute to knowledge about genotypic-phenotypic associations of *PRPH2* retinopathies and inform clinical and therapeutic end points.

Keywords: pattern dystrophy (PD), macular dystrophy, genetic sequencing, multimodal retinal imaging, *PRPH2*, peripherin-2 gene

Diagnosis of retinal and macular degenerations or dystrophies can be clinically challenging due to overlapping or atypical phenotypes, especially in the late stages of the disease. Late onset Stargardt disease with macular atrophy and geographic atrophy (GA) secondary to age-related macular degeneration (AMD) may have similar clinical presentations, but retinal flecks that may be present in Stargardt disease are not a typical feature in AMD. Pattern dystrophies (PDs) of the retinal pigment epithelium (RPE) with macular pigmentary abnormalities[1,2] may resemble AMD, but various other forms of RPE abnormalities that occur in PD might deviate from AMD diagnostic criteria. Retinal atrophy that is not confined to the macula and extends beyond the vascular arcades may also suggest a diagnosis other than AMD. Nonetheless, some cases of these retinopathies are misdiagnosed as AMD and may be inadvertently included in clinical studies specific for AMD. Utilizing multimodal retinal imaging beyond color fundus photography (CFP) can be helpful to distinguish characteristic features that are relevant for the differential diagnosis of these conditions, including fundus autofluorescence (FAF), near infrared reflectance (IR), and optical coherence tomography (OCT) imaging. Family history, age of onset, and genetic sequencing may also aid in the differential diagnosis of these conditions.

In this study, we selected individuals from our longitudinal database who presented with macular abnormalities in the clinical spectrum of differential diagnosis of AMD, but

were likely to carry genetic variants other than those related to AMD due to their low genetic susceptibility to AMD and/or relatively younger age of onset.[3–7] We investigated genetic variants associated with retinopathies using genetic sequencing methods and identified two peripherin-2 gene (*PRPH2*) or retina degeneration slow (RDS) OMIM #179605 variants in affected families and independent cases.[8,9] We present herein longitudinal results for a missense and splice-site *PRPH2* variant in three families and five independent cases using whole exome sequencing, multimodal imaging, and visual acuity scores, and describe the genotypic-phenotypic correlations which may further improve diagnostic accuracy. Preliminary results were presented at the Association for Research in Vision and Ophthalmology meeting in 2017[10] and the American Academy of Ophthalmology meeting in 2018.

Methods

Study Population and Subject Selection

All participants were enrolled in ongoing genetic and epidemiologic studies of AMD and retinal dystrophies, and were followed prospectively to determine the course of disease and visual outcomes (the Seddon Longitudinal Cohort Study or SLCS).[11] From the SLCS database, probands and family members were selected if at least one family member had low polygenic risk scores for AMD, as determined by a composite of genes known to predict AMD.[7] This suggested that the clinical phenotypes could be unrelated to AMD and possibly due to other genetic variants.[3–7,12,13] Other inclusion criteria included macular disease that did not conform to typical AMD presentation in at least one family member, such as relatively younger age of onset compared to AMD. Probands and family members were excluded if affected relatives carried known rare variants related to AMD, as previously reported, including *CFH* R1210C, *CFH* R53G, *CFH* D90G, *CFH* P503A, and *C3* K155Q and *C9* P167S.[5,6,14] Based on these selection criteria, 263 individuals including 59 families and unrelated individuals were selected for whole exome sequencing (WES).

The research protocol received approval from institutional review boards and all research adhered to the tenets of the Declaration of Helsinki. Written informed consent was obtained from all participants.

Ocular Examinations and Phenotyping

Participants underwent comprehensive ocular examinations conducted by board-certified ophthalmologists. These included a funduscopic examination, CFP, FAF, IR, fluorescein angiography (FA), OCT, and OCT angiography (OCTA) with Heidelberg Spectralis (Heidelberg Engineering, Heidelberg, Germany), Zeiss Cirrus (Carl Zeiss Meditec AG, Jena, Germany), and/or Optovue RTVue XR Avanti (Optovue Inc., Fremont, CA, USA). Expert retina specialists and image graders (authors J.M.S. and D.F.) evaluated multimodal retinal images to determine the presence, location, and overall aspect of the following imaging biomarkers: drusen or lipofuscin deposition; RPE abnormalities; RPE, retinal and choroidal atrophy; and any signs of macular neovascularization (NV). Eyes were classified according to the Clinical Age-Related Maculopathy Staging (CARMS) system at the time of enrollment and subsequent follow-up in SLCS, based on size of drusen and pigmentary abnormalities: 1 = no AMD; 2 = early AMD, or 3 = intermediate AMD; 4 = central or non-central atrophy corresponding to complete RPE and outer retinal atrophy; and 5 = retinal and subretinal NV disease.[15] Macular signs not typical of AMD, such as retinal degenerations and macular dystrophies, were classified as grade 6.

Genetic Sample Preparation and Whole Exome Sequencing

Genomic DNA was extracted from the blood of all individuals using a standard protocol. WES was performed.[5,6] The exomic sequence was targeted following the SureSelectXT Target Enrichment System for Illumina Paired-End Sequencing Library 6.1 protocol from Agilent. Following the exome library preparation, the samples were sequenced using the Illumina HiSeq2000 Sequencing System. The sequenced samples had an average of 96.6% of the exome covered at ≥ 10 times.

Read Mapping, Variant Detection, and Annotation

Following deconvolution of barcodes from each lane, individual reads were aligned to the human reference genome (hg19) using the Burrows-Wheeler Aligner, resulting in BAM files.[16] Variant calling was performed using the best recommendations from the tools present in the Genome Analysis Toolkit (GATK) version 3.1 suite.[17–19] For each sample, distinct genomic variant call format files (gVCF) containing variant calls for all loci were created using the HaplotypeCaller tool. The gVCFs were combined, and joint genotyping was performed across individuals using the GenotypeGVCFs tool. The resulting raw genotype calls in the VCF file were filtered for low-quality genotypes using the Variant Quality Score Recalibration tool. Other than high-quality variants assigned "PASS" by variant quality score recalibration (VQSR), we also included only those variants in lower tranches with truth sensitivity between 99.0 and 100 that were also separately recorded in the exome sequencing project database of 6500 samples.[20] After filtering, 598,065 high-quality variants were identified. Functional effects for the variants were annotated using the Ensembl Variant Effect Predictor.[21]

Variant Classification

To screen for rare genetic variants that segregated with macular diseases within these families, we used the xBrowse (https://xbrowse.broadinstitute.org) tool to filter variants in a stepwise manner. We prioritized variants that fulfilled the following criteria: (1) were rare (minor allele frequency [MAF] < 0.1%) in the 1000 Genomes Project and the ExAC databases), (2) belonged to a potentially damaging functional annotation class (i.e. nonsense, missense, splice site, and frameshift), (3) were predicted to impact protein function (i.e. in silico prediction of damaging or deleterious by PolyPhen-2,[22] SIFT,[23] MutationTaster2,[24] FATHMM,[25] and Human Splicing Finder[26] depending on the type of mutation), and (4) followed the inheritance pattern of disease within each family. In some cases, we performed Sanger sequencing or targeted sequencing after identifying potential causative variants in the WES, as previously described.[5,6,14]

Investigative Ophthalmology & Visual Science

Targeted Sequencing

A custom SureSelectXT Kit was used to capture genomic sequences of coding exons, splice junctions, 5′ UTR, and 3′ UTR regions in the selected genes with indexing barcodes for each sample. Hybridized library fragments were isolated, quantitated by qPCR and sequenced as paired-end reads with the Illumina HiSeq2000 sequencing platform. We required sequencing data for each sample to have over 10× coverage at greater than 90% targeted regions and over 20× coverage at greater than 80% targeted regions. Sequences were aligned to the human reference genome (NCBI build 37.3, hg19) with BWA (version 0.59).[16] We called the consensus genotypes in the target regions with GATK version 2.18 with the workflow and parameters recommended in the best practice variant detection with GATK version 4.[17,27] We applied GATK duplicate removal, indel realignment, base quality score recalibration, and performed multi-sample SNP and indel discovery and genotyping across all samples simultaneously using VQSR. Other than high-quality variants assigned "PASS" by VQSR, we also included only those variants in lower tranches with truth sensitivity between 99.0 and 100 that were also separately recorded in the exome sequencing project database of 6500 samples.[20] Variant annotation was performed with snpEff (version 2.05).[28] We further excluded SNPs failing the Hardy-Weinberg test in controls ($P < 10-6$) and alleles that had high missing genotype data (>1%), likely due to systematic low coverage or difficulty mapping reads across many samples. We also excluded samples with high missing genotype data (>1%) for common alleles with >1% frequency in our data set. For burden testing, we only tested those genes on autosomes that obtained >10× coverage at an average of >90% of the targeted region and had rare coding variants.

Assessment of Other Known Pathogenic Variants of Retinal Dystrophies

To confirm that the disease observed in these individuals was not the result of another known variant associated with retinal dystrophies, we checked for the presence of risk alleles for known pathogenic and rare novel variants in *BEST1*, *ABCA4*, *CTNNA1*, *IMPG1*, and *IMPG2*. This was done using the exome and targeted sequencing data. Although none of the individuals in this study were clinically diagnosed with retinitis pigmentosa (RP), we also checked for the presence of *ROM1* Gly80 (1-base pair insertions) and *ROM1* Leu114 (1-base pair insertions) known to be inherited with the *PRPH2* L185P variant in patients affected with digenic RP.[8]

Visual Acuity Analyses

Best corrected visual acuity (BCVA) scores were extracted from medical records during the clinical course of the

Table 1. Functional Interpretation of *PRPH2* Variants Associated With AMD Status

Gene	dbSNP ID	Chr	Position (Hg19)	Function	cDNA Position	CADD	PolyPhen2 (Score)	ClinVar Interpretation*	Minor/Major	MAF (GnomAD)
PRPH2	rs121918563	6	42689519	Missense p.Leu185Pro	c.554T>C	29.3	Probably damaging (1.0)	Pathogenic/likely pathogenic	G/A	1.4×10^{-5}
PRPH2	rs281865373	6	42672100	Splice-site variant IVS2+3A>T	c.828+3A>T	31.0	NA	Pathogenic	A/T	3.2×10^{-6}

Chr, chromosome; MAF, minor allele frequency; cDNA, complementary DNA; CADD, combined annotation-dependent depletion; NA, not applicable; gnomAD, Genome Aggregation Database.
* Retrieved January 16, 2024.

Table 2. Filtering of Variants in Exome Sequencing Data

	Number of Variants	
	Pedigree A	Pedigree B
MAF < 0.1% in databases	2018	1769
Shared among affected but not unaffected	90	263
High and moderate impact SNPs	20	8
Missense and nonsense variants		
Total	18	1
Probably damaging (Polyphen-2)	5	0
Deleterious (SIFT)	7	1
Disease causing (MutationTaster2)	11	1
Damaging (FATHMM)	4	0
Deleterious according to all four prediction software programs	1	0
Deleterious according to at least 3/4 prediction software programs	4*	0
Splice site variants		
Total	0	2
Disease causing (MutationTaster2)	NA	1
Affects splicing (Human Splicing Finder)	NA	2
Deleterious according to both prediction software programs	NA	1*

FATHMM, Functional Analysis through Hidden Markov Models; MAF, minor allele frequency; SIFT, sorting intolerant from tolerant; SNP, single-nucleotide polymorphism.
* Represents the candidate variant which might cause disease in the families.

Investigative Ophthalmology & Visual Science

Table 3. Demographic, Clinical, and Genetic Characteristics of Pedigree A With *PRPH2* Rare Variant rs121918563 (L185P)

ID	Sex	Age at Diagnosis or Earliest Clinical Record of Disease, Years	AMD Polygenic Risk Score	*PRPH2* Variant - Genotype	Baseline Visual Acuity (OD; OS)	Last Known Visual Acuity (OD; OS) and Follow-Up Time,* Years	Phenotypic Category	Ocular Phenotypic Description
Pedigree A carrying *PRPH2* mutation L185P, rs121918563								
A:I:1	M	56	0.23	A/G	20/40; 20/40	20/40; 20/40 (0)	Pattern dystrophy - AVMD	RPE abnormalities in the central macular area OU, with pigment clumping and small foveal area of RPE atrophy OD, and pseudo-vitelliform lesion typical of AVMD OS
A:II:1	M	51	2.35	A/G	20/25; 20/25	CF; 20/70 (11)	Pattern Dystrophy - AVMD	Pattern dystrophy presenting as AVMD OU. OD developed a retinal detachment which was repaired surgically. OS showed progressive absorption of pseudo-vitelliform lesion over time, evolving to a foveal area of RPE and outer retinal atrophy
A:II:2	M	39	2.35	A/A	20/20; 20/25	20/20; 20/25 (10)	Normal macula	Normal macula
A:II:3	F	39	1.83	A/G	20/50; 20/40	20/50; 20/60 (21)	Pattern dystrophy - AVMD	Central macular RPE changes with pattern configuration and RPE and outer retinal atrophy involving the fovea OU; no drusen. *ABCA4* variant (R943Q) identified by sequencing

ABCA4, ATP binding cassette subfamily A member 4 gene; AVMD, adult-onset vitelliform macular dystrophy; CF, count fingers visual acuity; OD, right eye; OS, left eye; OU, both eyes; *PRPH2*, peripherin-2 gene; RPE, retinal pigment epithelium.

*Follow-up time based on study enrollment dates.

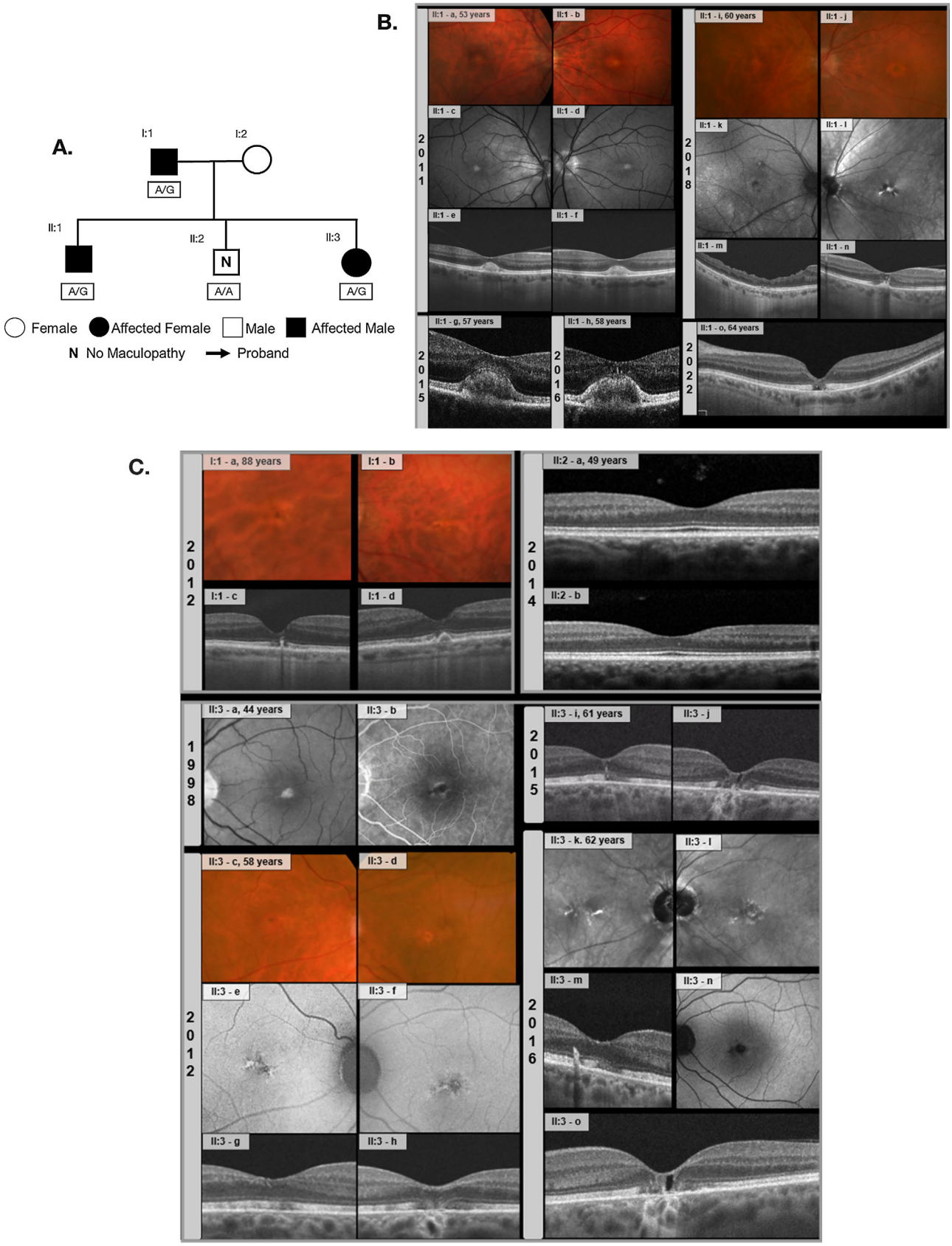

Figure 1. (**A**) Pedigree A, heterozygous for the *PRPH2* rare variant rs121918563 (L185P). (**B**) Phenotypes of Proband II:1 (*arrow* in **A**). (**a, b**) Small round yellowish lesion in the center of the macula in both eyes typical of PD presenting as AVMD on CFP. (**c, d**) Red-free retinography documenting the same central macular lesions in OU. (**e, f**) OCT with dense hyper-reflective material accumulation in the subretinal space in a vitelliform pattern, typical of AVMD. (**g, h**) Ultra-high resolution OCT shows pseudo-vitelliform lesions OU with

Investigative Ophthalmology & Visual Science

heterogeneous material, and RPE migration at the dome of the pseudo-vitelliform lesions (**h**). (**i, j**) CFP 7 years after baseline. (**k, l**) FAF OD showing mottled hyper and hypo-autofluorescence, and near IR OS showing pigmentary accumulation and clumping, associated with the pseudo-vitelliform lesions typical of AVMD in the center of the macula OU. (**m, n**) OCT shows thinning and disruption of the retinal layers and disappearance of the foveal lesion OD after a retinal detachment repair, and typical pseudo-vitelliform lesion in the center of the macula OS. (**o**) OCT OS, 11 years after baseline showing RPE abnormalities and outer retinal atrophy, likely secondary to natural history of the pseudo-vitelliform lesion. (**C**) Phenotypes of other family members in Pedigree A. I:1 (**a, b**) CFP and (**c, d**) OCT of proband's father showing central macular pseudo-vitelliform lesions in different stages OU typical of AVMD. II:2 (**a, b**) Normal OCT OU from sibling of proband without the variant. II:3 (**a–o**) Multimodal retinal imaging of the sister of the proband. (**a**) Red free and (**b**) FA at baseline showing central foveal lesions typical of AVMD. Images 14 years later include (**c, d**) CFP, (**e, f**) FAF, and (**g, h**) OCT showing RPE and outer retina irregularities including pigmentary clumping in both eyes and incipient central macular atrophy in the OS, typical of AVMD. (**i–o**) OCT and IR images 17 to 18 years after baseline show RPE irregularities in a pattern configuration, with RPE and outer retina atrophy OU. AVMD, adult-onset vitelliform macular dystrophy; CFP, color fundus photography; FA, fluorescein angiography; FAF, fundus autofluorescence; IR, infrared reflectance; OCT, optical coherence tomography; OD, right eye; OS, left eye; OU, both eyes; *PRPH2*, peripherin-2 gene; RPE, retinal pigment epithelium.

disease and was converted to logarithm of the minimal angle of resolution (logMAR). Distributions of initial and final visual acuity (logMAR) for each genetic variant were plotted where the width of each violin plot is proportional to the density for the range of values. For the longitudinal analysis, we ran mixed effects linear regression, with a compound symmetry correlation structure to account for the correlation between fellow eyes to assess the rate of change of visual acuity (logMAR) over time (1 line of Snellen vision = 0.1 logMAR). The regression model included time (years), genetic variant, and the cross product of time × genetic variants. For this analysis, we censored an eye if it reached BCVA of counting fingers or worse at a particular clinical visit. We calculated the change in visual acuity (logMAR) per year for each genetic variant.

Results

Overview

We identified two *PRPH2* rare variants rs121918563 L185P (p.Leu185Pro, c.554T>C) and splice-site rs281865373 c.828+3A>T (IVS2+3A>T; Table 1) in 22 individuals (44 eyes), all with retinal diffuse and/or macular abnormalities, among which 17 were members of 3 families and 5 were independent cases. The genotypic and phenotypic characterizations of a total of 25 individuals (50 eyes), including 3 additional family members with no *PRPH2* variants and no abnormalities on fundus exam, are described herein.

Fourteen of the 25 individuals (56%) were women, and all were of European ancestry. The mean age at diagnoses or the earliest clinical record for individuals with the *PRPH2* L185P variant was 56 years ($n = 7$, range = 39–66 years) and the mean age of individuals with the *PRPH2* c.828+3A>T variant was 48 years ($n = 15$, range = 24–70 years). Among those with longitudinal data, the mean follow-up time was 14 years (range = 1–27 years).

Familial Phenotype of *PRPH2* rs121918563 L185P (p.Leu185Pro, c.554T≥C)

Pedigree A. Four individuals in this two-generation family were enrolled in the study. Genetic analysis of this family under the hypothesis of an autosomal dominant inherited coding variant revealed a list of 20 variants. Due to the disease prevalence in this family, we narrowed our search to coding variants that are predicted to have a deleterious effect on the protein, with a resulting list of only 4 variants: *TAS1R2* L581P, *ANGPT1* R493Q, *THBD* R106C, and *PRPH2* L185P (Table 2). Of note, from this small list, we identified the missense variant in *PRPH2*, rs121918563, a transition from adenine to guanine that leads to a change from leucine to proline at amino acid 185 (*PRPH2* L185P).[8]

There were 3 affected individuals with the heterozygous *PRPH2* L185P variant (Table 3; Fig. 1), including the proband (II:1), his sister (II:3), and his father (I:1). All of these individuals exhibited macular abnormalities compatible with PD. Notably, both the proband and the father had manifestations of adult-onset vitelliform macular dystrophy (AVMD) displaying bilateral and symmetric well delineated, circular, yellowish pseudo-vitelliform lesions in the center of the macula measuring less than one disc diameter, surrounded by pigmentary abnormalities. The proband's sister had pigmentary clumping in the center of the macular area typical of PD. The proband's brother did not have this variant (II:2) and had a normal fundus examination.

None of the members of this family had any known pathogenic or other rare variants in *BEST1*, *IMPG1*, or *IMPG2*, nor did they carry either of the *ROM1* variants known to be carried by patients with digenic RP. The sister of the proband (II:3), heterozygous for L185P, also had the *ABCA4* R943Q variant (rs1801581). This *ABCA4* missense variant has conflicting reports of pathogenicity in ClinVar. It has been noted in patients diagnosed with AMD, Stargardt disease, and in individuals who have no clinical manifestations of retinal disease.[29]

Familial Phenotype of *PRPH2* Splice-Site rs281865373 c.828±3A≥T (IVS2±3A≥T)

Pedigree B. This 3-generation family had 13 individuals enrolled in the study. Analysis of this family began by conducting WES on five affected members (II:4, II:8, II:10, III:3, and III:6). When considering all members as affected with the same disease, the inheritance pattern was autosomal dominant. After filtering out variants not shared by all sequenced members, common variants, and variants from classes not expected to have an impact on the protein, eight variants remained (see Table 2). After this, only one variant was predicted to be damaging by multiple prediction software. This variant, rs281865373, is a thymine to adenine transversion in the *PRPH2* gene within the splice donor site between exons 2 and 3 (*PRPH2* c.828+3A>T). After identifying this variant, we used Sanger sequencing to genotype the remaining members of Pedigree B, including unaffected family members to confirm that the variant segregated with the disease.

Investigative Ophthalmology & Visual Science

Table 4. Demographic, Clinical, and Genetic Characteristics of Pedigree B With *PRPH2* Rare Variant rs281865373 (c.828+3A>T)

ID	Sex	Age at Diagnosis or Earliest Clinical Record of Disease, Years	AMD Polygenic Risk Score	*PRPH2* Variant - Genotype	Baseline Visual Acuity (OD; OS)	Last Known Visual Acuity (OD; OS) and Follow-Up Time* Years	Phenotypic Category	Ocular Phenotypic Description
Pedigree B carrying *PRPH2* mutation c.828+3A>T, rs281865373								
B:II:1	M	Unknown	0.42	A/T	20/200; 20/200	20/200; 20/200 (0)	CACD	Central atrophy extending to vascular arcades OU
B:II:4	F	41	0.29	A/T	20/25; 20/30	20/50; 20/30 (13)	Central atrophy	Scattered mottled RPE hypopigmentation in macula and temporal to macula OU at age 80 (no images)
B:II:5	F	89	−0.67	A/A	20/20; 20/25	20/40; 20/30 (13)	Normal macula	Normal macula, unaffected; no maculopathy documented by photography
B:II:7	F	51	−0.64	A/T	20/30; 20/40	20/30; 20/80 (12)	CACD	Macular and peripapillary atrophy, extending beyond the retinal vascular arcades and worsening during follow up period OU
B:II:8	F	24	−0.89	A/T	20/50; 20/200	20/100; CF (3)	CACD	Macular and peripapillary atrophy, extending beyond the retinal vascular arcades and worsening during follow up period OU
B:II:10	F	37	0.51	A/T	20/25; 20/100	20/70; CF (21)	CACD	Large areas of retinal atrophy evolved to extensive atrophy involving macula and extending beyond the retinal vascular arcades OU
B:III:2	F	52	1.43	A/T	20/30; 20/40	20/60; 20/70 (20)	AFMD with central atrophy	Yellow flecks in the macular area and extending beyond the retinal vascular arcades resembling AFMD present at baseline; similar to daughter (IV: I) at the same age. Symmetric, large areas of central RPE atrophy developed during follow-up OU
B:III:3	F	48	−0.84	A/T	20/30; 20/30	20/400; 20/80 (20)	AFMD with central atrophy	Yellow flecks in the macular area and extending beyond the retinal vascular arcades present at baseline (age 56). Evolved to central macular atrophy resembling GA secondary to AMD in OU, and secondary macular NV OU treated with multiple injections of anti-VEGF, showing residual intraretinal fluid (age 67)
B:III:4	M	49	1.59	A/T	20/25; 20/25	CF; 20/50 (26)	AFMD with central atrophy	Macular atrophy with foveal sparing resembling GA secondary to AMD in OU at baseline, which evolved to large central retinal atrophy OU over 19 y of follow up
B:III:5	F	36	1.11	A/T	20/20; 20/50	CF; 20/250 (27)	Central atrophy	Large areas of macular atrophy and subretinal fibrosis secondary to macular NV OU
B:III:6	M	49	0.67	A/T	20/25; 20/50	CF; 20/200 (14)	CACD	Lipofuscin deposits in the macular area and central atrophy resembling GA secondary to AMD in OU at baseline, which progressed to extensive retinal atrophy affecting the macular area and extending beyond the retinal vascular arcades OU over 14 y of follow up
B:III:7	M	50	0.63	A/T	20/40; 20/400	20/60; CF (1)	AFMD with central atrophy	Yellow flecks in the macular area and extending beyond the retinal vascular arcades and central macular atrophy OU. Secondary macular NV OU
B:IV:1	F	40	1.55	A/T	20/50; 20/32	20/50; 20/32 (0)	AFMD	Yellow flecks in the macular area and extending beyond the retinal vascular arcades OU

AFMD, adult-onset fundus flavimaculatus with macular dystrophy; AMD, age-related macular degeneration; CACD, central areolar chorioretinal dystrophy; CF, count fingers visual acuity; GA, geographic atrophy; NV, neovascularization; OD, right eye; OS, left eye; OU, both eyes; *PRPH2*, peripherin-2 gene; RPE, retinal pigment epithelium.

* Follow-up time based on study enrollment dates.

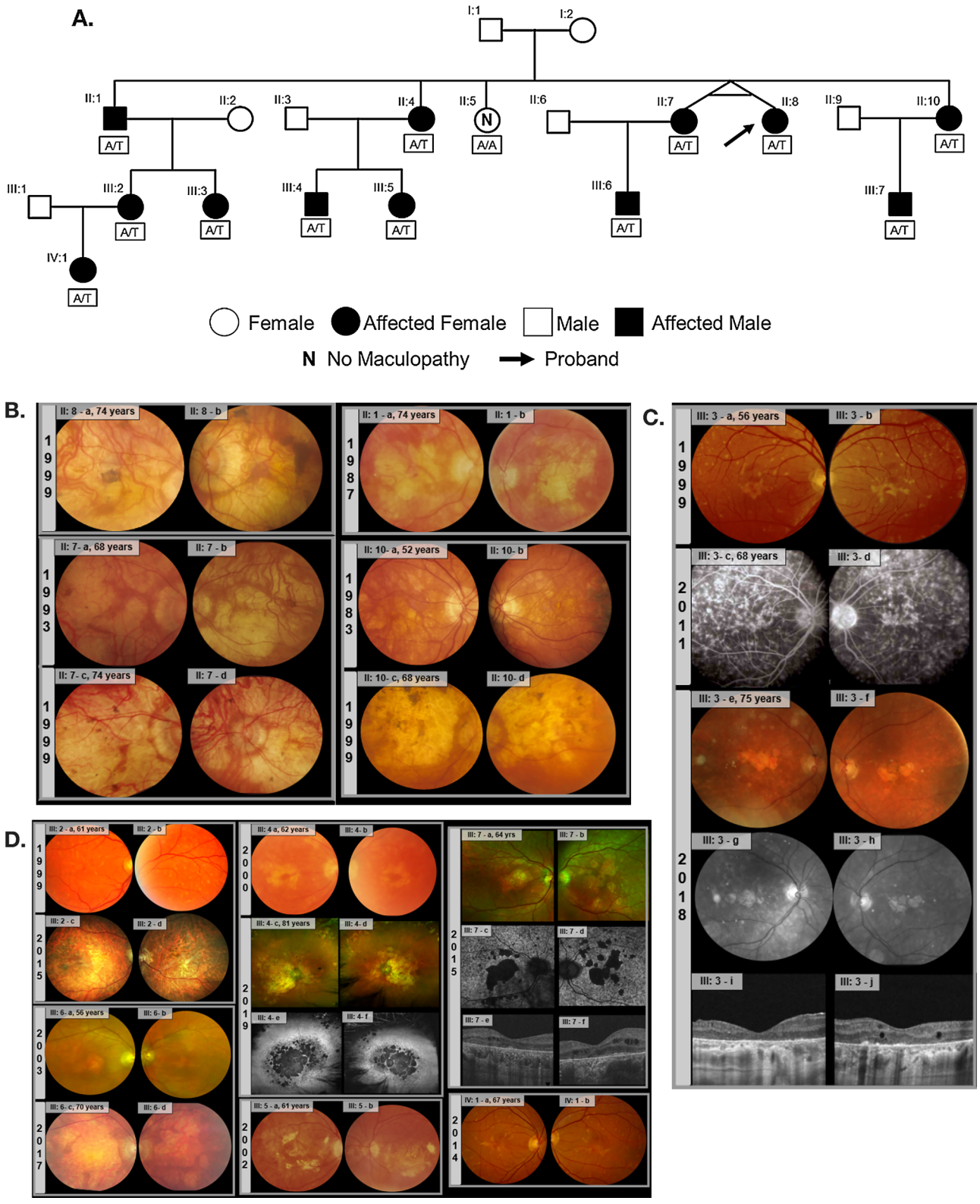

Figure 2. (**A**) Pedigree B, heterozygous for the *PRPH2* rs281865373 (c.828+3A>T) variant. (**B**) Phenotypes of proband II:8 (*arrow* in **A**) and identical twin sister (II:7). Proband II:8 (**a, b**) CFP shows bilateral extensive macular and peripapillary retinal atrophy extending beyond the retinal vascular arcades, consistent with CACD. II:7 Identical twin of the proband. (**a–d**) CFP shows a very similar clinical presentation in comparison to the proband, with further worsening of the diffuse retinal atrophy over a follow-up time of 6 years. II:1 Sibling of the proband. (**a, b**) Large areas of retinal and RPE atrophy extending throughout the macula (CACD). II:10 Sibling of the proband. (**a–d**) CFP OU show patches of retinal atrophy in the central macula evolving over a period of 16 years to retinal atrophy involving the entire macular area and extending to the retinal vascular arcades (CACD). (**C**) III:3 Niece of proband. (**a–i**) Multimodal retinal imaging from baseline to 19 years of follow-up shows yellow retinal flecks as seen in AFMD on (**a, b**) CFP and (**c, d**) FA. Central macular atrophy resembling GA secondary to AMD developed over a follow-up time of 19 years as seen in (**e, f**) CFP and (**g, h**) red-free retinography. (**i, j**) Last documentation with

Investigative Ophthalmology & Visual Science

OCT shows outer retinal atrophy throughout the macula OU and residual intraretinal fluid OS after intravitreal anti-vascular endothelial growth factor for secondary macular NV OU. (**D**) Other nieces and nephews of the proband and 1 great-niece. III:2 Niece of proband. (**a–d**) CFP demonstrates RPE irregularities and retinal flecks resembling AFMD, which progressed over a period of 16 years to large areas of retinal atrophy affecting the macular area and extending beyond the retinal vascular arcades in OU. III:6 Nephew of the proband. (**a–d**) CFP OU show central area of macular atrophy that resembles GA secondary to AMD, which evolved over a follow-up time of 14 years to develop extensive retinal atrophy throughout the macular area and extending beyond the retinal vascular arcades, more typical of CACD. III:4 Nephew of the proband. (**a, b**) CFP OU show central macular atrophy that resemble GA secondary to AMD with foveal sparing, which evolved over 19 years to more widespread retinal atrophy extending nasally to the optic nerve and in the far retinal periphery, as shown on (**c, d**) CFP and (**e, f**) FAF. III:5 Niece of the proband. (**a, b**) CFP OU exhibits large areas of macular atrophy and subretinal fibrosis involving the central macular area with history of bilateral macular NV. III:7 Nephew of the proband. (**a, b**) CFP and (**c, d**) FAF show central macular atrophy and significant abnormalities of the retina and RPE extending throughout the macular area and beyond the retinal vascular arcades OU. (**e, f**) OCT shows outer retinal atrophy and intraretinal cystic spaces in both eyes. IV:1 Daughter of III:2. (**a, b**) CFP OU show retinal flecks as seen on AFMD at baseline. AFMD, adult-onset fundus flavimaculatus with macular dystrophy; AMD, age-related macular degeneration; CACD, central areolar chorioretinal dystrophy; CFP, color fundus photographs; FA, fluorescein angiography; FAF, fundus autofluorescence; GA, geographic atrophy; NV, neovascularization; OCT, optical coherence tomography; OS, left eye; OU, both eyes; *PRPH2*, peripherin-2 gene; RPE, retinal pigment epithelium.

Twelve of the 13 family members had the *PRPH2* c.828+3A>T heterozygous variant and all were clinically affected (Table 4; Fig. 2). The proband (II:8), her identical twin (II:7), and 3 siblings (II:1, II:4, II:10) had this *PRPH2* splice-site variant. They exhibited diffuse RPE abnormalities and macular atrophy, and, in some cases, RPE atrophy extended beyond the retinal vascular arcades (see Fig. 2), whereas the sibling (II:5) was the only wild-type individual and had a normal fundus examination. The son of the proband (III:6), five of her nieces and nephews (III:2–7), and a grandniece (IV:1) also had the variant and were clinically affected, four of whom (III:2, III:3, III:6, and IV:1) presented with yellow flecks in the macular area extending throughout the temporal retinal vascular arcades, consistent with adult-onset fundus flavimaculatus with macular dystrophy (AFMD). Over time, multimodal retinal imaging showed disease progression starting from diffuse atrophy of the retina and the RPE, advancing to the macular area and extending beyond the retinal vascular arcades throughout the posterior pole. This was consistent with central areolar chorioretinal dystrophy (CACD), among the cases with or without retinal flecks that had follow-up records available. Two nieces (III:3 and III:5) and one nephew (III:7) also developed macular NV.

Thus, we confirmed the variant was exclusively present in the affected family members. None of the family members had any known pathogenic or other rare variants in *ABCA4*, *BEST1*, *CTNNA1*, *IMPG1*, *IMPG2*, or *ROM1*.

Pedigree C. Given the known phenotypic presentations of the *PRPH2* variants identified in Pedigrees A and B, we searched all previously collected genetic data for individuals in our database to identify additional individuals with *PRPH2* variants. A query of our targeted sequencing data identified one subject who was initially diagnosed with GA secondary to AMD based on clinical examination (II:2) and was heterozygous for *PRPH2* c.828+3A>T. This subject was part of an expanded family unit within our database for which we had phenotypic and genetic data on two additional siblings. Investigating these 3 sisters, 2 were heterozygous for the *PRPH2* c.828+3A>T variant and were also clinically affected (Table 5; Fig. 3). The proband (II:1) showed macular atrophy in both eyes that could be misdiagnosed as GA secondary to AMD but showed RPE abnormalities in spoke-like configuration in the central macular area more prominent in one eye, which is more commonly seen in PD. The area of macular atrophy enlarged over 7 years in both eyes. Similarly, the proband's sister (II:2) had a comparable phenotype with macular atrophy and enlargement of the lesions in both eyes over 15 years. The other sister (II:3) did not have this variant and had a normal fundus examination.

Phenotypic Presentation of Independent Cases

Five independent cases were also determined to be heterozygous for the *PRPH2* variants by genetic sequencing. Four were heterozygous for the *PRPH2* L185P variant (cases A to D), one individual was heterozygous for the splice-site variant *PRPH2* c.828+3A>T (case E), and all 5 cases were clinically affected (Table 6; Fig. 4). Some cases were initially misdiagnosed as GA secondary to AMD before being referred to our study, and one of them had been previously enrolled in a clinical trial for AMD.

All four affected individuals (cases A to D) with the *PRPH2* L185P variant had fundus features typical of PD, similar to Pedigree A. Two cases (A and D) presented with macular abnormalities typical of PD in their 60s which evolved to the central area of macular atrophy in their 70s. Two other cases (B and C) demonstrated the so-called butterfly shaped presentation of PD with a central area of macular atrophy. In case C, the OCTA revealed type 1 macular NV adjacent to the area of RPE atrophy in both eyes, which was not suspected based on clinical history but was associated with shallow, low-lying RPE detachment on OCT. Case D also presented with central areas of macular atrophy and developed exudative macular NV in both eyes.

One individual who was heterozygous for *PRPH2* c.828+3A>T (case E) evolved to extensive atrophy of the retina and RPE in both eyes, similar to some phenotypes observed in Pedigrees B and C with the same variant. This subject presented at baseline with bilateral, multifocal areas of macular atrophy which enlarged to central and paracentral retinal atrophy in both eyes, and which could clinically resemble GA secondary to AMD at this stage. Over a follow-up period of 10 years, the atrophic lesions progressed beyond the topography of the retinal vascular arcades and posterior pole consistent with CACD, based on clinical records.

None of these independent cases have any known pathogenic or other rare variants in *BEST1*, *CTNNA1*, *IMPG1*, or *IMPG2*, and *ROM1* variants. One of these individuals (case B) was heterozygous for *ABCA4* V2050L (rs41292677), a rare missense variant listed as having uncertain significance as per American College of Medical Genetics and Genomics (ACMG) criteria in ClinVar.[30,31] This variant has been reported as a genetic modifier seen in conjunction with

Investigative Ophthalmology & Visual Science

Investigative Ophthalmology & Visual Science

Table 5. Demographic, Clinical, and Genetic Characteristics of Pedigree C With *PRPH2* Rare Variant rs281865373 (c.828+3A>T)

ID	Sex	Age at Diagnosis or Earliest Clinical Record of Disease (Yrs)	AMD Polygenic Risk Score	*PRPH2* Variant - Genotype	Baseline Visual Acuity (OD; OS)	Last Known Visual Acuity (OD; OS) and Follow-Up Time* Years	Phenotypic Category	Ocular Phenotypic Description
Pedigree C carrying *PRPH2* mutation c.828+3A>T, rs281865373								
C:II:1	F	70	0.99	A/T	20/200; 20/40	20/200; 20/100 (7)	Pattern dystrophy and central atrophy	Central macular atrophy OU resembling GA secondary to AMD. RPE abnormalities in spoke-like configuration more evident in one eye; absence of drusen OU.
C:II:2	F	63	1.31	A/T	20/60; 20/30	CF; 20/400 (15)	Central atrophy	Central macular atrophy OU resembling GA secondary to AMD, with enlargement during follow up
C:II:3	F	70	2.18	A/A	20/30; 20/25	20/25; 20/25 (19)	Normal macula	Normal macula

AMD, age-related macular degeneration; CF, count fingers visual acuity; GA, geographic atrophy; OD, right eye; OS, left eye; OU, both eyes; *PRPH2*, peripherin-2 gene; RPE, retinal pigment epithelium.
*Follow-up time based on study enrollment dates.

PRPH2 R172W and *ROM1* variants, but not with the *PRPH2* L185P variant present in this subject.[32]

Best Corrected Visual Acuity Results

Figure 5 displays distribution of visual acuity in both variants at the initial and final visits and trends during the follow-up period. Visual acuity (logMAR) in individuals with the *PRPH2* c.828+3A>T variant was worse at the final visit compared to the initial visit, whereas less vision loss from baseline was seen in individuals heterozygous for L185P (see Fig. 5A). For individuals heterozygous for *PRPH2* c.828+3A>T, visual acuity change per year was +0.021 (±0.006), and for individuals heterozygous for *PRPH2* L185P the slope was +0.006 (±0.005; see Fig. 5B). Therefore, a greater rate of vision loss for the *PRPH2* splice site variant was observed, aligning with more severe phenotypes seen in affected individuals carrying this variant compared to the missense variant ($P < 0.001$ for difference in rates of decline over time between the two variants). Because the first BCVA measurement in this study was collected once the macular abnormalities were already clinically significant, and medical records are not available at the onset of their retinal disease, the overarching impact of the genetic variants on rate of visual decline may be underestimated.

Discussion

In this study, we used whole exome sequencing to explore genetic underpinnings of maculopathies and we identified two *PRPH2* genetic mutations (L185P and c.828+3A>T) in unrelated families and independent cases, which were not explained by other variants. Genotypic-phenotypic evaluation with longitudinal multimodal imaging revealed varied clinical manifestations described in PD or CACD. Some cases showed variable clinical manifestation throughout the follow-up period and some evolved to macular atrophy with or without macular NV over time, underscoring the importance of accurate diagnoses enabled by next generation sequencing, especially for maculopathies associated with earlier onset or other clinical features atypical for AMD. These results provide additional information about the natural history associated with these variants which have been classified as likely pathogenic/pathogenic using the 2015 ACMG criteria in ClinVar (www.ncbi.nih.gov/clinvar),[33,34] and the Human Gene Mutation Database (www.hgmd.cf.ac.uk).[35]

Clinical Manifestations of the *PRPH2* Variants

The phenotypes were meaningfully different between the two *PRPH2* variants, whereas they were more similar but not identical within each variant. Retinal abnormalities described in this study included clinical manifestations characteristic of PD, such as AVMD, AFMD, and CACD. In all individuals with the *PRPH2* L185P variant (rs121918563), fundus findings typical of PD were observed. Some affected individuals with the L185P variant had AVMD which developed in their 40s and 50s which evolved to RPE irregularities and central areas of macular atrophy in their mid-60s. Others exhibited PD which presented as butterfly shaped RPE irregularities that evolved to small areas of central macular atrophy in their 70s. A few individuals later developed macular NV. Two cases with the L185P variant each had a different

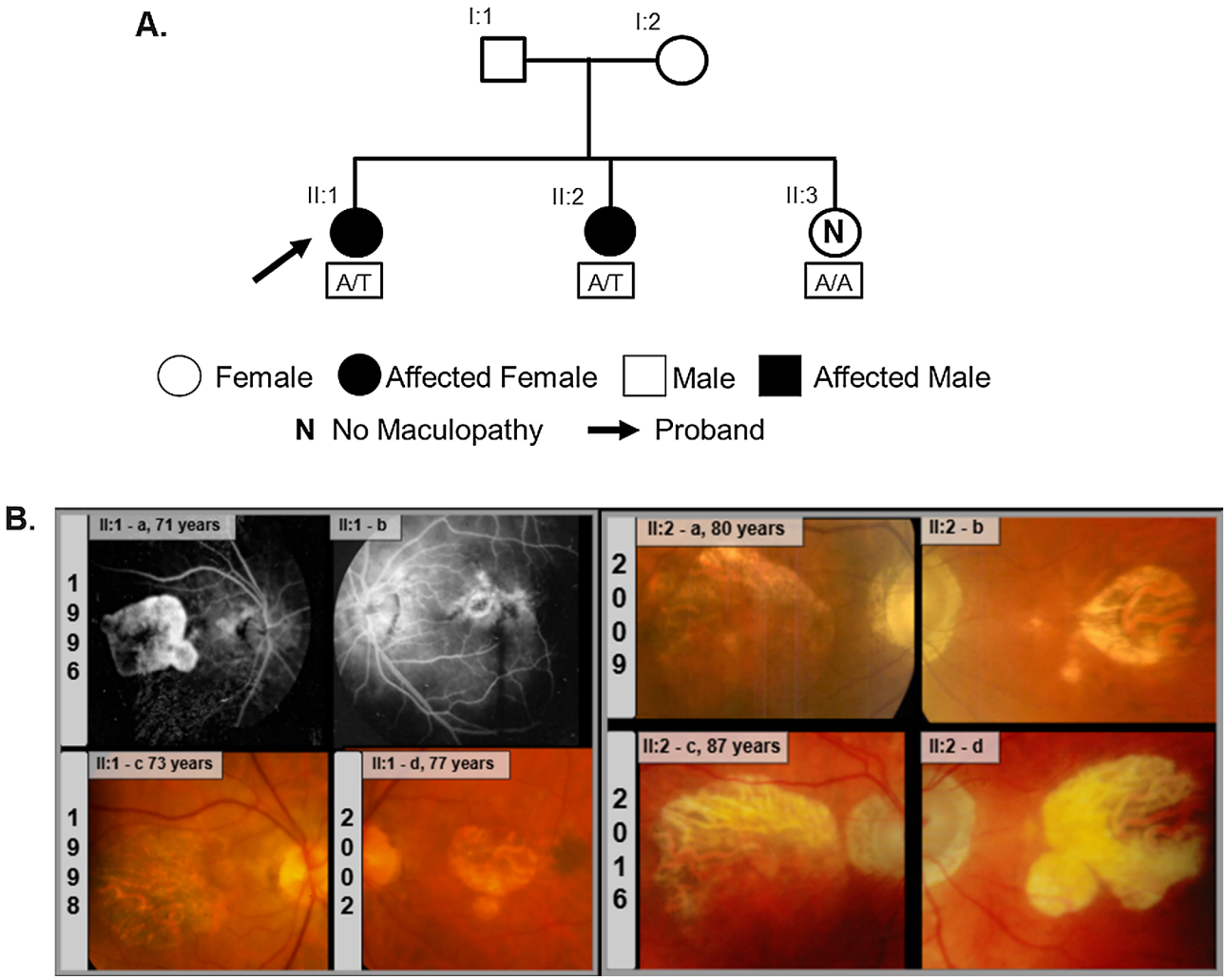

Figure 3. (**A**) Pedigree C, heterozygous for the *PRPH2* rs281865373 (c.828+3A>T) variant. (**B**) Phenotypes of Proband II:1. (**a, b**) FA OU shows central macular atrophy that may resemble GA secondary to AMD, but with RPE abnormalities in spoke-like configuration similar to pattern dystrophy more evident OS. (**c, d**) CFP OU demonstrates worsening of central macular atrophy that could be confounded with GA secondary to AMD but also fit in the differential diagnosis of early CACD. II:2 Sibling of the Proband. (**a–d**) CFP OU exhibits clinical presentation very similar to the Proband, with central macular atrophy in the differential diagnosis of GA secondary to AMD or CACD, with enlargement of the lesions 7 years after baseline. AMD, age-related macular degeneration; CACD, central areolar chorioretinal dystrophy; CFP, color fundus photographs; FA, fluorescein angiography; GA, geographic atrophy; OS, left eye; OU, both eyes; *PRPH2*, peripherin-2 gene; RPE, retinal pigment epithelium.

ABCA4 variant, which may have affected the severity of the phenotypes, however, neither case had retinal flecks which can occur with fundus flavimaculatus or Stargardt disease. In summary, all individuals with the L185P variant in our study manifested various clinical presentations of PD, evolving over time to macular areas of RPE and outer retinal atrophy.

Affected individuals with the *PRPH2* c.828+3A>T splice-site variant (rs281865373) exhibited a different phenotype with more diffuse RPE and outer retinal atrophy worsening over time, and some were consistent with CACD. Some individuals had flecks, such as fundus flavimaculatus and/or multifocal areas of retinal atrophy confined to the macula in their early 50's. These lesions further evolved to diffuse retinal atrophy, extending beyond the macula and the topography of retinal vascular arcades in their late 60s to 80s. Phenotypes associated with this splice-site variant resemble those reported in a cross-sectional study.[36] In our longitudinal study, one individual with the splice-site variant had a presentation of PD, as seen in some individuals with the L185P variant.

Another correlation between genotype and phenotype was the degree of visual acuity decline over time. Individuals with the splice-site variant had more severe visual loss over the follow-up period. In contrast, individuals with the missense L185P variant had mild to moderate visual impairment over time. The trends for differences in retinopathies and visual outcomes suggest patterns that warrant further investigation to inform clinical trial end points.

Previous Literature About *PRPH2* Variants

There are numerous reported *PRPH2* variants and many have been associated with retinal disorders[37–41] including PD,[42–44] RP,[8,45] CACD,[36,46,47] retinitis punctata albescens,[48] cone-rod dystrophy,[49,50] AMD-like late-onset maculopathy,[51]

Table 6. Demographic, Clinical, and Genetic Characteristics of Independent Cases With *PRPH2* Rare Variants

ID	Sex	Age at Diagnosis or Earliest Clinical Record of Disease Years	AMD Polygenic Risk Score	*PRPH2* Variant - Genotype	Baseline Visual Acuity (OD; OS)	Last Known Visual Acuity (OD; OS) and Follow-up Time * Years	Phenotypic Category	Ocular Phenotypic Description
Independent Cases carrying *PRPH2* mutation L185P, rs121918563								
Case A	F	52	−2.65	A/G	20/50; 20/20	20/60; 20/20 (10)	Pattern dystrophy AVMD	Foveal pseudo-vitelliform lesions OU at baseline, which were absorbed and progressed to small foveal areas of RPE and outer retinal atrophy OU over 8 y follow up
Case B	M	64	−0.66	A/G	20/30; 20/250	20/30; 20/320 (5)	Pattern dystrophy butterfly and central atrophy	RPE irregularities in butterfly configuration OD; central atrophy OS. *ABCA4* variant (V2050L) identified by sequencing
Case C	M	62	1.38	A/G	20/30; 20/30	20/30; 20/25 (11)	Pattern dystrophy central atrophy and NV	RPE irregularities in butterfly configuration with small areas of central macular atrophy, with secondary non-exudative macular NV OU
Case D	M	66	−0.49	A/G	20/60; 20/20	CF; 20/25 (17)	Pattern dystrophy central atrophy and NV	RPE defects in butterfly configuration OU; progressed to central small areas of macular atrophy and NV OU over 9 y follow up
Independent Case carrying *PRPH2* mutation c.828+3A>T, rs281865373								
Case E	M	62	1.2	A/T	20/20; 20/400	20/200; CF (10)	CACD	Areas of macular atrophy that enlarged over time and extended beyond the topography of retinal vascular arcades OU

ABCA4, ATP binding cassette subfamily A member 4 gene; AVMD, adult-onset vitelliform macular dystrophy; CACD, central areolar chorioretinal dystrophy; CF, count fingers visual acuity; NV, neovascularization; *PRPH2*, peripherin-2 gene; RPE, retinal pigment epithelium.

* Follow-up time based on study enrollment dates.

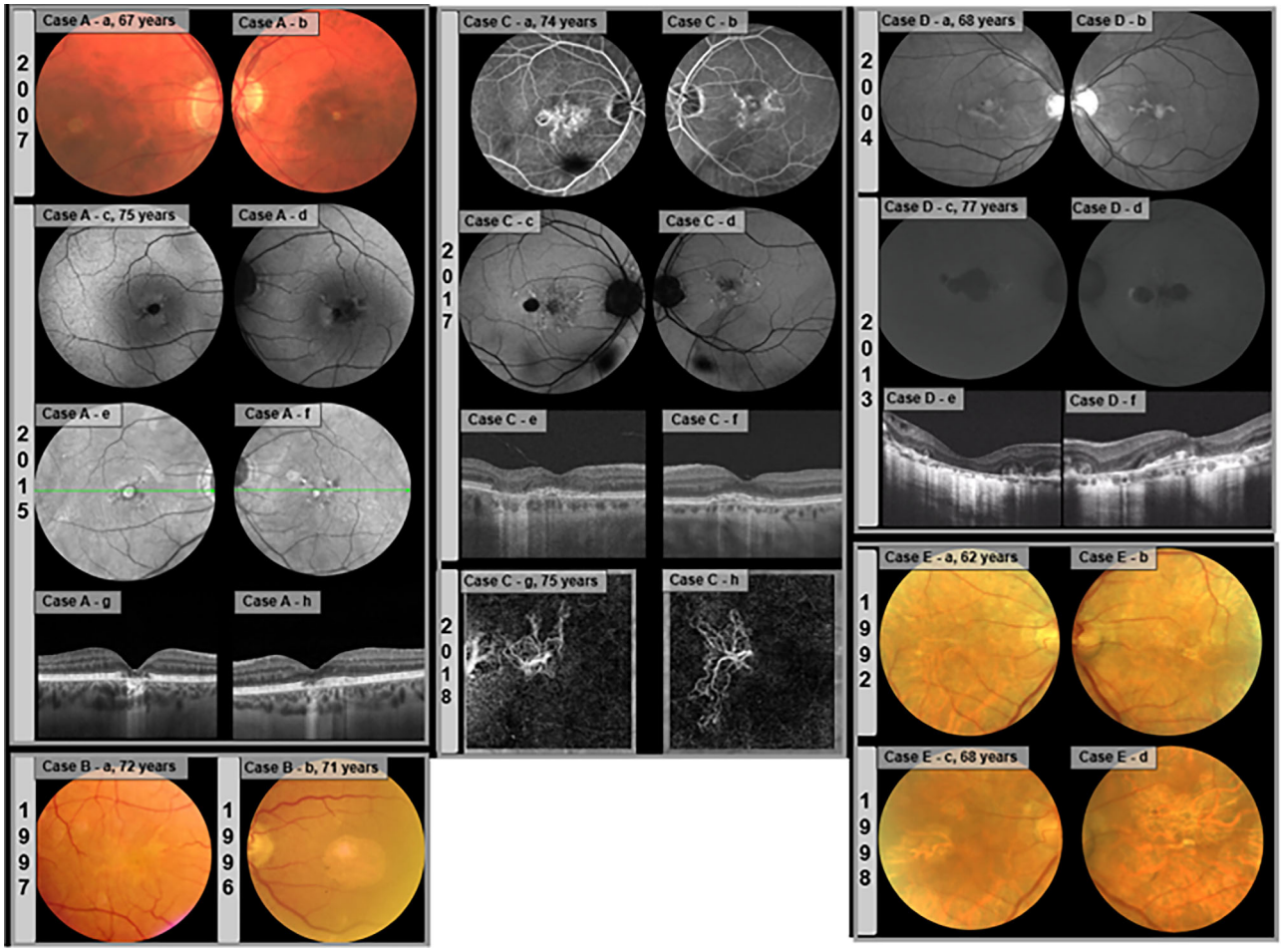

Figure 4. Phenotypes of independent cases, heterozygous for the *PRPH2* rs121918563 (L185P) variant (cases A—D) and the *PRPH2* rs281865373 (c.828+3A>T) variant (case E). Case A. (**a, b**) CFP OU show central pseudo-vitelliform macular lesions which evolved to small circular area of central RPE and outer retinal atrophy, also shown on (**c, d**) fundus autofluorescence (FAF) and (**e, f**) near IR as well as on (**g, h**) OCT typical of AVMD. Of note, IR images show a pattern configuration of pigmentary clumps. Case B. (**a, b**) CFP exhibits RPE irregularities in a butterfly shape OD and central atrophy OS. Case C. (**a, b**) FA OU show small central macular atrophy surrounded by increased fluorescence due to pigmentary mobilization and marked fluorescein staining, and (**c, d**) FAF OU shows small areas of distinct hypo-autofluorescence correspondent to the central macular atrophy, and increased areas of FAF in a distinct butterfly pattern correspondent to the areas of pigmentary mobilization. (**e, f**) OCT OU show small focal areas of RPE and outer retinal atrophy, and shallow "low-lying" RPE detachments in both eyes, without evident signs of exudation. (**g, h**) OCTA OU show macular NV. Case D. (**a, b**) Red-free retinography in both eyes show RPE abnormalities in a butterfly pattern configuration. (**c, d**) FAF OU show progression to central macular atrophy 9 years after baseline, and in the same visit (**e, f**) OCT OU show central macular atrophy and subretinal fibrosis secondary to macular NV. Case E. (**a, b**) CFP OU show multifocal areas of RPE atrophy. (**c, d**) CFP OU show that 6 years after baseline the areas of macular atrophy enlarged, resembling GA secondary to AMD earlier in the disease presentation but that could fit in the differential diagnosis of CACD as the disease progressed. AMD, age-related macular degeneration; CACD, central areolar chorioretinal dystrophy; CFP, color fundus photographs; FA, fluorescein angiography; FAF, fundus autofluorescence; GA, geographic atrophy; IR, infrared reflectance; NV, neovascularization; OCT, optical coherence tomography; OCTA, optical coherence tomography angiography; OD, right eye; OS, left eye; OU, both eyes; *PRPH2*, peripherin-2 gene; RPE, retinal pigment epithelium.

and Leber congenital amaurosis.[52] The splice site variant c.828+3A>T is one of the most common *PRPH2* variants and has been shown to exhibit variable expressivity similar to what we have reported,[36,37,53,54] whereas the missense L185P is less common.[41,45,54–56] Of note, a vast spectrum of *PRPH2* variants and phenotypic presentations (including those reported in this paper) have been reported and/or reviewed by Sears et al. (2001),[37] Boon et al. (2008),[38] Shankar et al. (2015-16),[36,53] Reeves et al. (2020),[54] Peeters et al. (2021),[41] and Heath Jeffrey et al. (2024).[57]

Genomics for *PRPH2* Gene and Genetic Mutations

The *PRPH2* gene encodes the protein Peripherin-2 and consists of 3 exons located on Chromosome 6p21. The protein is membrane-associated glycoprotein crucial for photoreceptor outer segment function.

The *PRPH2* L185P variant is located in the second intradiscal loop of the protein, the portion of the protein where over 70% of disease-causing variants are located. This loop is vital to the formation of *PRPH2* homotetramers and *PRPH2/ROM1* heterotetramers, the impairment of which results in abnormal disc morphogenesis, photoreceptor degeneration, and subsequent visual loss.[58,59] Another study showed that when the *PRPH2* L185P was expressed by itself in COS-1 cells, it was unable to form homotetramers, but when expressed along with wild type ROM1 protein, the *PRPH2* L185P mutant proteins were still able to form heterotetramers.[60] These heterotetramers are involved in the formation of a higher-order complex that extends over the

Investigative Ophthalmology & Visual Science

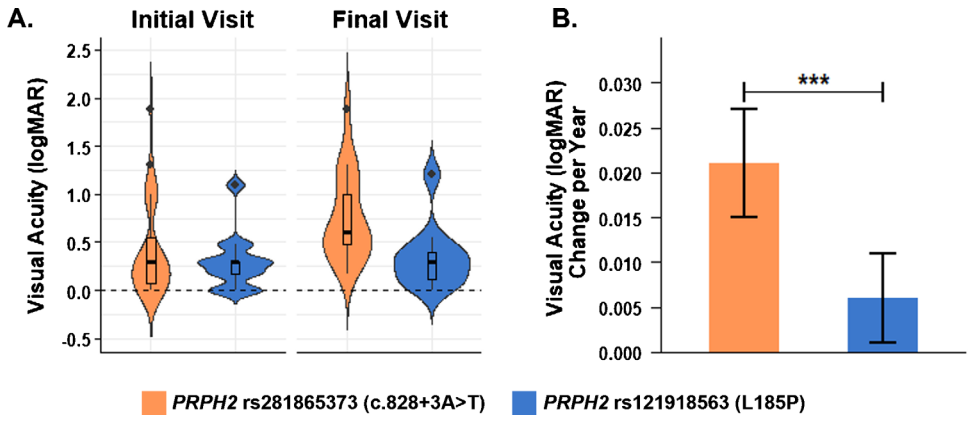

Figure 5. (**A**) Violin plots showing initial and final visual acuity (logMAR) for individuals heterozygous for *PRPH2* rs281865373 (c.828+3A>T) (*orange*) and *PRPH2* rs121918563 (L185P) (*blue*) variants. The width of each violin plot is proportional to the density for the range of values and the medians are represented by *horizontal bars* within the boxplots. (**B**) Comparison of change in visual acuity (logMAR) per year between individuals heterozygous for *PRPH2* rs281865373 (c.828+3A>T) (*orange*) and *PRPH2* rs121918563 (L185P) (*blue*) estimated using a mixed effects linear regression with a compound symmetry correlation structure. Standard error is illustrated by *vertical error bars* (***$P < 0.001$). logMAR, logarithm of the minimal angle of resolution; *PRPH2*, peripherin-2 gene.

entire circumference of the disc.[61] The individuals in this study have the *PRPH2* L185P variant but are wild type at the positions in *ROM1* known to cause digenic RP. We hypothesize that individuals who carry *PRPH2* L185P are able to form heterotetramers with *ROM1*, but are unable to form the higher-order complexes consisting of both homo- and heterotetramers.[61] This inability to form homotetramers, and in turn higher-order complexes, may result in the manifestations of PD seen in Pedigree A and four independent cases. Modifier genes could also explain variable phenotypes and different penetrance in patients with the same variant described in this study.

The other variant described in this report, *PRPH2* c.828+3A>T, is a splice-site variant located between the second and third exons and leads to the addition of 10 amino acids to exon 2 and then a stop codon is encountered. This premature stop results in the last exon being absent from the protein. This last exon encodes the final piece of the protein that is located within the discal membrane and the C terminal of the protein that is in the cytoplasmic space. So, this variant leads to the formation of a nonfunctional truncated protein. It is considered pathogenic as per reports in ClinVar and HGMD.[33–35]

Strengths and Limitations

Strengths of this study include the identification of protein-coding variants using whole exome genetic sequencing, although non-coding regions would not be detected. The SLCS database enabled us to determine families and independent individuals with *PRPH2* retinopathies who had the variants and to assess differences in phenotypes. This comprehensive evaluation with longitudinal clinical examinations and multimodal retinal imaging provides further insights into the natural history of disease progression, benefited also by remarkably long follow-up periods in some cases. Our results also contribute to the body of knowledge on differential diagnosis of retinal dystrophies and AMD, which could be crucial for evaluation of new therapeutics. Limitations include acquisition of ocular data from a study database augmented by real-world clinical care at variable follow-up times. The cohort with *PRPH2* variants was relatively small and electrophysiological findings were not available for most cases.

Conclusions

In conclusion, this report underscores important clinical phenotypic features associated with variants of the *PRPH2* gene and demonstrates the autosomal dominant pattern of inheritance with variable expressivity. There was a trend for individuals with the same variant to have similar phenotypes and visual outcomes, with more marked differences seen between the two variants. Results contribute to the characterization of clinically heterogeneous cases of *PRPH2* retinopathies associated with two distinct variants of the gene, adds information about the natural untreated course of these diseases, and provides new information about their visual outcomes over time. Detailed clinical assessment paired with comprehensive genetic analysis is integral for accurate diagnosis, and for a better understanding of the natural history and underlying pathophysiology of inherited retinal disorders, with relevance for both clinical research and clinical practice.

Acknowledgments

The authors thank Bernard Rosner, PhD, for his statistical advice, William Casazza, PhD, for review of the manuscript, and Luis Nakayama, MD, for assistance with literature review.

Supported in part by National Institutes of Health, National Eye Institute R01-EY011309, R01-EY028602, Bethesda, MD; Carl Marshall Reeves and Mildred Almen Reeves Foundation, Inc., Fenton, MO; American Macular Degeneration Foundation, Northampton, MA; Macular Degeneration Center of Excellence, University of Massachusetts Chan Medical School, Department of Ophthalmology and Visual Sciences, Worcester, MA. The sponsor or funding organization had no role in the design or conduct of this research.

Disclosure: **J.M. Seddon**, Gemini Therapeutics (I), Apellis Pharmaceuticals (I), Laboratoires Théa, Inc. (C); **D. De**, None; **L. Grunenkovaite**, None; **D. Ferrara**, Roche (I), Genentech, Inc. (E)

References

1. Gass JDM. Stereoscopic Atlas of Macular Diseases: Diagnosis and Treatment. *JAMA*. 1997;277:1411–1412.
2. Pattern Dystrophies - EyeWiki. Accessed January 29, 2024. Available at: https://eyewiki.org/Pattern_Dystrophies.
3. Sobrin L, Maller JB, Neale BM, et al. Genetic profile for five common variants associated with age-related macular degeneration in densely affected families: a novel analytic approach. *Eur J Hum Genet*. 2010;18(4):496–501.
4. Yu Y, Reynolds R, Rosner B, Daly MJ, Seddon JM. Prospective assessment of genetic effects on progression to different stages of age-related macular degeneration using multistate Markov models. *Invest Ophthalmol Vis Sci*. 2012;53(3):1548–1556.
5. Yu Y, Triebwasser MP, Wong EKS, et al. Whole-exome sequencing identifies rare, functional CFH variants in families with macular degeneration. *Hum Mol Genet*. 2014;23(19):5283–5293.
6. Wagner EK, Raychaudhuri S, Villalonga MB, et al. Mapping rare, deleterious mutations in Factor H: association with early onset, drusen burden, and lower antigenic levels in familial AMD. *Sci Rep*. 2016;6:31531.
7. Huan T, Cheng SY, Tian B, et al. Identifying novel genes and variants in immune and coagulation pathways associated with macular degeneration. *Ophthalmol Sci*. 2023;3(1):100206.
8. Kajiwara K, Berson EL, Dryja TP. Digenic retinitis pigmentosa due to mutations at the unlinked peripherin/RDS and ROM1 loci. *Science*. 1994;264(5165):1604–1608.
9. Sohocki MM, Daiger SP, Bowne SJ, et al. Prevalence of mutations causing retinitis pigmentosa and other inherited retinopathies. *Hum Mutat*. 2001;17(1):42–51.
10. Villalonga MB, Collins GK, Silver RE, Seddon JM. Peripherin-2 mutations identified by whole exome sequencing in clinically heterogeneous families with retinal pattern dystrophies. *Invest Ophthalmol Vis Sci*. 2017;58(8):2777.
11. Seddon JM. Macular degeneration epidemiology: nature-nurture, lifestyle factors, genetic risk, and gene-environment interactions – the Weisenfeld Award Lecture. *Invest Ophthalmol Vis Sci*. 2017;58(14):6513–6528.
12. Yu Y, Reynolds R, Fagerness J, Rosner B, Daly MJ, Seddon JM. Association of variants in the LIPC and ABCA1 genes with intermediate and large drusen and advanced age-related macular degeneration. *Invest Ophthalmol Vis Sci*. 2011;52(7):4663–4670.
13. Yu Y, Bhangale TR, Fagerness J, et al. Common variants near FRK/COL10A1 and VEGFA are associated with advanced age-related macular degeneration. *Hum Mol Genet*. 2011;20(18):3699–3709.
14. Seddon JM, Yu Y, Miller EC, et al. Rare variants in CFI, C3 and C9 are associated with high risk of advanced age-related macular degeneration. *Nat Genet*. 2013;45(11):1366–1370.
15. Seddon JM, Sharma S, Adelman RA. Evaluation of the clinical age-related maculopathy staging system. *Ophthalmology*. 2006;113(2):260–266.
16. Li H, Durbin R. Fast and accurate short read alignment with Burrows-Wheeler transform. *Bioinforma Oxf Engl*. 2009;25(14):1754–1760.
17. McKenna A, Hanna M, Banks E, et al. The Genome Analysis Toolkit: a MapReduce framework for analyzing next-generation DNA sequencing data. *Genome Res*. 2010;20(9):1297–1303.
18. Van der Auwera GA, Carneiro MO, Hartl C, et al. From FastQ data to high confidence variant calls: the Genome Analysis Toolkit best practices pipeline. *Curr Protoc Bioinforma*. 2013;43(1110):11.10.1–11.10.33.
19. Genome Analysis Toolkit (GATK). Accessed March 22, 2023. Available at: https://gatk.broadinstitute.org/hc/en-us.
20. Tennessen JA, Bigham AW, O'Connor TD, et al. Evolution and functional impact of rare coding variation from deep sequencing of human exomes. *Science*. 2012;337(6090):64–69.
21. McLaren W, Pritchard B, Rios D, Chen Y, Flicek P, Cunningham F. Deriving the consequences of genomic variants with the Ensembl API and SNP Effect Predictor. *Bioinforma Oxf Engl*. 2010;26(16):2069–2070.
22. Adzhubei IA, Schmidt S, Peshkin L, et al. A method and server for predicting damaging missense mutations. *Nat Methods*. 2010;7(4):248–249.
23. Ng PC, Henikoff S. Predicting deleterious amino acid substitutions. *Genome Res*. 2001;11(5):863–874.
24. Schwarz JM, Cooper DN, Schuelke M, Seelow D. MutationTaster2: mutation prediction for the deep-sequencing age. *Nat Methods*. 2014;11(4):361–362.
25. Shihab HA, Gough J, Mort M, Cooper DN, Day INM, Gaunt TR. Ranking non-synonymous single nucleotide polymorphisms based on disease concepts. *Hum Genomics*. 2014;8(1):11.
26. Desmet FO, Hamroun D, Lalande M, Collod-Béroud G, Claustres M, Béroud C. Human Splicing Finder: an online bioinformatics tool to predict splicing signals. *Nucleic Acids Res*. 2009;37(9):e67.
27. DePristo MA, Banks E, Poplin R, et al. A framework for variation discovery and genotyping using next-generation DNA sequencing data. *Nat Genet*. 2011;43(5):491–498.
28. Cingolani P, Platts A, Wang LL, et al. A program for annotating and predicting the effects of single nucleotide polymorphisms, SnpEff: SNPs in the genome of Drosophila melanogaster strain w1118; iso-2; iso-3. *Fly (Austin)*. 2012;6(2):80–92.
29. VCV000007913.34 - ClinVar - NCBI. Accessed September 12, 2023. Available at: https://www.ncbi.nlm.nih.gov/clinvar/variation/7913/.
30. VCV000007884.48 - ClinVar - NCBI. Accessed November 7, 2023. Available at: https://www.ncbi.nlm.nih.gov/clinvar/variation/7884/.
31. Richards S, Aziz N, Bale S, et al. Standards and guidelines for the interpretation of sequence variants: a joint consensus recommendation of the American College of Medical Genetics and Genomics and the Association for Molecular Pathology. *Genet Med Off J Am Coll Med Genet*. 2015;17(5):405–424.
32. Poloschek CM, Bach M, Lagrèze WA, et al. ABCA4 and ROM1: implications for modification of the PRPH2-associated macular dystrophy phenotype. *Invest Ophthalmol Vis Sci*. 2010;51(8):4253–4265.
33. VCV000013165.11 - ClinVar - NCBI. Accessed January 22, 2024. Available at: https://www.ncbi.nlm.nih.gov/clinvar/variation/13165/?oq=((28204[AlleleID]))&m=NM_000322.5(PRPH2):c.554T%3EC%20(p.Leu185Pro).
34. VCV000098713.21 - ClinVar - NCBI. Accessed January 22, 2024. Available at: https://www.ncbi.nlm.nih.gov/clinvar/variation/98713/.
35. The Human Gene Mutation Database: building a comprehensive mutation repository for clinical and molecular genetics, diagnostic testing and personalized genomic medicine - PubMed. Accessed October 15, 2024. Available at: https://pubmed-ncbi-nlm-nih-gov.umassmed.idm.oclc.org/24077912/.
36. Shankar SP, Hughbanks-Wheaton DK, Birch DG, et al. Autosomal dominant retinal dystrophies caused by a founder splice site mutation, c.828+3A>T, in PRPH2 and protein haplotypes in trans as modifiers. *Invest Ophthalmol Vis Sci*. 2016;57(2):349–359.
37. Sears JE, Aaberg TA, Daiger SP, Moshfeghi DM. Splice site mutation in the peripherin/RDS gene associated

with pattern dystrophy of the retina. *Am J Ophthalmol*. 2001;132(5):693–699.
38. Boon CJF, den Hollander AI, Hoyng CB, Cremers FPM, Klevering BJ, Keunen JEE. The spectrum of retinal dystrophies caused by mutations in the peripherin/RDS gene. *Prog Retin Eye Res*. 2008;27(2):213–235.
39. Duncan JL, Talcott KE, Ratnam K, et al. Cone structure in retinal degeneration associated with mutations in the peripherin/RDS gene. *Invest Ophthalmol Vis Sci*. 2011;52(3):1557–1566.
40. Stuck MW, Conley SM, Naash MI. PRPH2/RDS and ROM-1: historical context, current views and future considerations. *Prog Retin Eye Res*. 2016;52:47–63.
41. Peeters MHCA, Khan M, Rooijakkers AAMB, et al. PRPH2 mutation update: In silico assessment of 245 reported and 7 novel variants in patients with retinal disease. *Hum Mutat*. 2021;42(12):1521–1547.
42. Marmor MF, Byers B. Pattern dystrophy of the pigment epithelium. *Am J Ophthalmol*. 1977;84(1):32–44.
43. Wells J, Wroblewski J, Keen J, et al. Mutations in the human retinal degeneration slow (RDS) gene can cause either retinitis pigmentosa or macular dystrophy. *Nat Genet*. 1993;3(3):213–218.
44. Nichols BE, Drack AV, Vandenburgh K, Kimura AE, Sheffield VC, Stone EM. A 2 base pair deletion in the RDS gene associated with butterfly-shaped pigment dystrophy of the fovea. *Hum Mol Genet*. 1993;2(5):601–603.
45. Kajiwara K, Hahn LB, Mukai S, Travis GH, Berson EL, Dryja TP. Mutations in the human retinal degeneration slow gene in autosomal dominant retinitis pigmentosa. *Nature*. 1991;354(6353):480–483.
46. Boon CJF, Klevering BJ, Cremers FPM, et al. Central areolar choroidal dystrophy. *Ophthalmology*. 2009;116(4):771–782, 782.e1.
47. Hoyng CB, Heutink P, Testers L, Pinckers A, Deutman AF, Oostra BA. Autosomal dominant central areolar choroidal dystrophy caused by a mutation in codon 142 in the peripherin/RDS gene. *Am J Ophthalmol*. 1996;121(6):623–629.
48. Kajiwara K, Sandberg MA, Berson EL, Dryja TP. A null mutation in the human peripherin/RDS gene in a family with autosomal dominant retinitis punctata albescens. *Nat Genet*. 1993;3(3):208–212.
49. Piguet B, Héon E, Munier FL, et al. Full characterization of the maculopathy associated with an Arg-172-Trp mutation in the RDS/peripherin gene. *Ophthalmic Genet*. 1996;17(4):175–186.
50. Kohl S, Christ-Adler M, Apfelstedt-Sylla E, et al. RDS/peripherin gene mutations are frequent causes of central retinal dystrophies. *J Med Genet*. 1997;34(8):620–626.
51. Khani SC, Karoukis AJ, Young JE, et al. Late-onset autosomal dominant macular dystrophy with choroidal neovascularization and nonexudative maculopathy associated with mutation in the RDS gene. *Invest Ophthalmol Vis Sci*. 2003;44(8):3570–3577.
52. Wang X, Wang H, Sun V, et al. Comprehensive molecular diagnosis of 179 Leber congenital amaurosis and juvenile retinitis pigmentosa patients by targeted next generation sequencing. *J Med Genet*. 2013;50(10):674–688.
53. Shankar SP, Birch DG, Ruiz RS, et al. Founder effect of a c.828+3A>T splice site mutation in peripherin 2 (PRPH2) causing autosomal dominant retinal dystrophies. *JAMA Ophthalmol*. 2015;133(5):511–517.
54. Reeves MJ, Goetz KE, Guan B, et al. Genotype-phenotype associations in a large PRPH2-related retinopathy cohort. *Hum Mutat*. 2020;41(9):1528–1539.
55. Coussa RG, Chakarova C, Ajlan R, et al. Genotype and phenotype studies in autosomal dominant retinitis pigmentosa (adRP) of the French Canadian Founder Population. *Invest Ophthalmol Vis Sci*. 2015;56(13):8297.
56. Sullivan LS, Bowne SJ, Birch DG, et al. Prevalence of disease-causing mutations in families with autosomal dominant retinitis pigmentosa: a screen of known genes in 200 families. *Invest Ophthalmol Vis Sci*. 2006;47(7):3052.
57. Heath Jeffery RC, Thompson JA, Lo J, et al. Retinal dystrophies associated with peripherin-2: genetic spectrum and novel clinical observations in 241 patients. *Invest Ophthalmol Vis Sci*. 2024;65(5):22.
58. Kedzierski W, Nusinowitz S, Birch D, et al. Deficiency of rds/peripherin causes photoreceptor death in mouse models of digenic and dominant retinitis pigmentosa. *Proc Natl Acad Sci USA*. 2001;98(14):7718–7723.
59. Loewen CJR, Moritz OL, Tam BM, Papermaster DS, Molday RS. The role of subunit assembly in peripherin-2 targeting to rod photoreceptor disk membranes and retinitis pigmentosa. *Mol Biol Cell*. 2003;14(8):3400–3413.
60. Goldberg AF, Molday RS. Defective subunit assembly underlies a digenic form of retinitis pigmentosa linked to mutations in peripherin/rds and rom-1. *Proc Natl Acad Sci USA*. 1996;93(24):13726–13730.
61. Kedzierski W, Weng J, Travis GH. Analysis of the rds/peripherin.rom1 complex in transgenic photoreceptors that express a chimeric protein. *J Biol Chem*. 1999;274(41):29181–29187.

Investigative Ophthalmology & Visual Science